2018 26th Mediterranean Conference on Control and Automation (MED)
Zadar, Croatia, June 19-22, 2018

Mid-ranging control concept for a multirotor UAV with moving masses

Tomislav Haus, Antun Ivanovic, Marko Car, Matko Orsag and Stjepan Bogdan

***Abstract*— This paper addresses the problem of actuators saturation that occur when one applies a moving mass concept to control the attitude of a multirotor UAV. In particular, we propose to combine the moving mass control (MMC) with rotors' variations in a paradigm known as a mid-ranging control. We show that this control structure ensures reference tracking and disturbance rejection with the moving masses operating in the middle of their range, which eventually reduces the possibility to violate their saturation limits. We also address the stability and design of the proposed controller by employing Routh-Hourwitz criterion and root-locus analysis. The controller is verified within a simulation environment, where we test its performance and compare it with a basic MMC concept under various disturbances. Finally, we present experimental results that we obtained with a modified ArduCopter vehicle, which serves as an experimental platform for the MMC verification.**

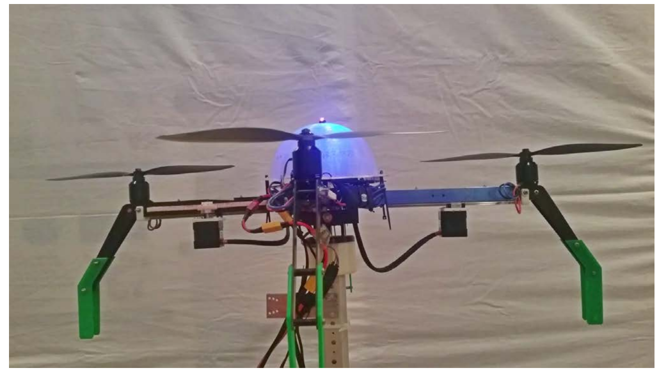

Fig. 1: Scaled down version of the MORUS UAV with moving mass control mechanism dubbed μMORUS. Only two masses equipping a single axis can be observed.

I. Introduction

In the last decade, the research on unmanned aerial vehicles (UAVs) has been one of the most active research fields in robotics, taking over the position of the wheeled robots that have dominated mobile robotics research before [1]. Multirotor UAVs have been the most popular research platforms, and among them, quadrotors have attracted the most interest due to their simple mechanical design, low cost, sufficient payload and flight time for various experimental scenarios. The first mathematical model of a quadrotor vehicle has been presented in 2002 [2]. Since then, extensive research has been conducted on development of novel estimation and control algorithms, as well as on practical applications of such vehicles. Nowadays, multirotor aerial vehicles are commercially used mostly for recording, surveillance and reconstruction, being equipped with conventional cameras, infra-red cameras and lasers. In more recent applications, large multirotor vehicles are being deployed in agriculture for spraying crops, a task that has earlier been dedicated to fixed wing aerial vehicles. At the same time, the research community has gone even further in applying such vehicles to challenging scenarios, equipping them with sensors and powerful onboard computers that provide autonomy in GPS-denied environments, and bringing them in contact with the environment. The most impressive scenarios include grasping and transporting objects [3], manipulating objects [4], conducting contact inspection [5] and constructing assemblies [6].

Within the MORUS project, we aim to further extend the field of applications of multirotor UAVs by bringing a UAV in a maritime environment to work closely with an Autonomous Underwater Vehicle (AUV). Since the project's missions require the multirotor UAV payload and flight time not available in the UAV market nowadays, we proposed to build an unmanned aerial vehicle powered with four internal combustion engines (ICE). In our previous work, we have shown that a Moving Mass Control (MMC) concept increases a controllability of such a vehicle by shifting the Center of Gravity (CoG) position, and thus achieving a fast and precise control of rolling and pitching moments, otherwise difficult to achieve with dynamically slow and inconsistent ICEs [7][8]. In this paper we go further with our control design and demonstrate how to use both moving masses and rotors' variations in order to control roll/pitch angles. We combine these two control concepts through a paradigm known as mid-ranging control. This paradigm has been introduced in process industry for plant control with multiple actuators working simultaneously [9],[10]. The main idea is to utilize faster actuators to achieve fine dynamical response and slower actuators to ensure that the faster actuators do not saturate. In recent years, this type of control has gained attention in robotics, in particular for position control of a robotic arm consisted of a macro and mini manipulator [11], [12]. We aim to use this concept for roll/pitch control of the MORUS UAV by utilizing ICE powered rotors

Authors are with Faculty of Electrical and Computer Engineering, University of Zagreb, 10000 Zagreb, Croatia (tomislav.haus, antun.ivanovic, marko.car, matko.orsag, stjepan.bogdan)@fer.hr

to compensate for slow disturbances and the moving masses to achieve the desired dynamical transients, while ensuring that the masses always work in the middle of their operating range.

The contribution of this paper is a design of the mid-ranging control algorithm based on Valve Position Control concept that we propose to use for our MORUS UAV. To the best of authors' knowledge, a mid-ranging control has not yet been used in a multirotor UAV control, and thus presents a completely novel approach in the field. We analyze the stability and performance of the vehicle controlled with the proposed concept (Section III), and we demonstrate the algorithm effectiveness in simulation (Section IV) and on an experimental tested (Section V). For experiments, we use a scaled model of the MORUS UAV dubbed μMORUS, shown in Fig. 1.

II. Related work

This paper extends on our work on the moving mass concept for attitude control of a multirotor UAV. In particular, in [7] we presented a 6DOF nonlinear dynamical model of the vehicle, and a linearized model in the form of transfer functions. In the same paper, we presented the heavy lift UAV with internal combustion engines and moving masses, dubbed MORUS UAV. For that vehicle, we gave the analysis of its static and dynamical characteristics as functions of the moving mass weight, maximum reach and dynamics, and we derived requirements on the moving mass parameters in order to ensure vehicle stability and desired robustness. Furthermore, we presented roll/pitch control design based on the classical cascade Proportional-Proportional (P-P) controller, and we gave a root-locus analysis to determine the controller's gains. The concept was tested both in simulation and on an experimental testbed consisted of the MORUS UAV mounted on a 2DOF gimbal.

In this paper, we utilize the linearized vehicle's model presented in [7]. In particular, the roll/pitch dynamics is the main focus of this paper, so we write the corresponding the transfer functions:

$$G_1(s) = \frac{\omega_y(s)}{x(s)} = \frac{2mg - 2m(1-4\mu)z_m s^2}{I_{yy}s(\frac{s^2}{\omega_{mm}^2} + \frac{2\zeta_{mm}}{\omega_{mm}}s + 1)}, \quad (1)$$

$$G_2(s) = \frac{\omega_y(s)}{\Delta\Omega(s)} = \frac{4b_f\Omega_0 L}{I_{yy}s(T_r s + 1)}, \quad (2)$$

where $G_1(s)$ describes pitch rate ($\omega_y(s)$) dynamics given a reference of the moving mass position ($x(s)$), and $G_2(s)$ presents pitch rate dynamics given a rotor variation reference ($\Delta\Omega(s)$). We follow the notation from our previous work, hence, m denotes the moving mass weight, μ as the ratio of the moving mass weight and the vehicle weight, g represents gravity constant, I_{yy} as the vehicle's moment of inertia in the pitch axis, z_m as the moving mass vertical displacement from the vehicle's body CoG (L_0 frame in [7]), ω_{mm} and ζ_{mm} as the servo system natural frequency and damping, b_f as the rotor thrust

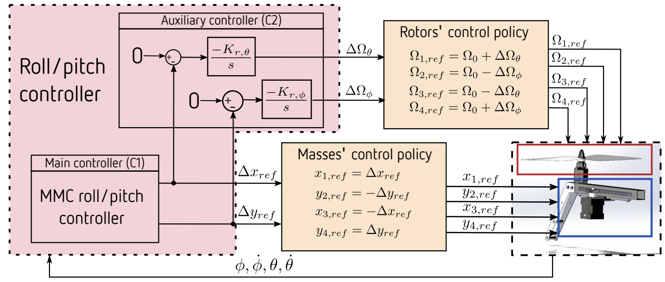

Fig. 2: The structure of the proposed MMC-VPC controller.

constant, L as the motor arm length, Ω_0 as the hovering velocity and T_r as the rotor's time constant.

We observed during the experiments that the main drawback of the MMC concept is the saturation of the moving masses in case of an existing disturbance in the roll or pitch axis. In particular, if we varied the thrust coefficient of a single rotor (e.g. ± 5 %) in simulation, it causes the shift of the moving masses' steady state positions closer to the arms' edges. Given an angle reference, the moving masses' position saturates in a transient phase, which deteriorates vehicle dynamical response and even causes instability. Similar effects were observed in a case of a wind gust disturbance applied to the vehicle.

During the experiments with the MORUS UAV on the gimbal, we observed disturbances coming from the gimbal friction and gravity force. The later was caused by a misalignment between the gimbal axis of rotation and the vehicle's CoG. If there was a horizontal displacement between the gimbal axis and vehicle's CoG, the moving masses's steady state position shifts from their nominal operating point (the middle of the motor arm). In case there was also a vertical displacement and the vehicle was commanded a constant roll/pitch reference, the moving masses are further displaced from their nominal operating point, and get closer to their saturation point. Motivated by these observations, in the next section we propose a novel control structure that keeps the moving masses' operating point in the middle of the motor arm regardless of disturbances or commanded attitude references.

III. Mid-ranging control concept

In this section we present a mid-ranging controller concept which utilizes both CoG positioning and rotors' variations to control vehicle's attitude. We propose to use a structure based on the Valve Position Control (VPC) concept [10]. The concept is named after a liquid flow control problem with a small and a big valve, where a big valve can produce higher flow than a small valve, but with less precision and slower response [9]. On the other hand, using only a small valve often results in actuator saturation and inability to satisfy flow capacities. VPC based control algorithm manipulates both valves to track desired flow level while keaping steady state value of the small valve at given setpoint.

For the MORUS UAV roll/pitch control concept, moving masses are considered as a small valve, while the rotors represent the big valve. We have shown in [7] that the MMC based control has higher bandwidth than the control based on rotors powered by IC engines. We also claim that rolling/pitching torques can be controlled with higher precision through MMC than with rotors' variations, since the MMC concept ideally controls the position of the CoG in a millimeter range. On the other hand, the torque that can be produced by rotors' variations is much larger than the maximum torque produced by shifting the CoG, which allows us to utilize it as the "big" valve. In this paper, we verify the VPC concept using the μMORUS vehicle (Fig. 1), emulating slow rotors by commanding slowly varying references for rotors powered with BLDC motors.

In the proposed concept (Fig. 2), the main controller (MMC) manipulates the position of the moving masses in order to track roll/pitch references. In this paper we utilize a cascade P-P MMC controller, but note that for the main controller we can utilize any type of a MMC controller, e.g. state space controller presented in [13]. The auxiliary controller (VPC) generates references for rotors' variations with a goal to keep the steady state position of the moving mass mechanism in the middle of its operating range. Note that the reference for this controller is 0, which is considered as a neutral position in this paper. The feedback signal of the VPC controller is the reference position of the vehicle's CoG generated by the MMC controller.

A. Reference tracking and disturbance rejection

In this paper we show important properties of the MMC-VPC controller for the linearized pitch dynamical model presented by the transfer functions (1) and (2). If we denote by C_1 the main MMC controller and by C_2 the auxilliary VPC controller, the closed loop transfer function of the vehicle's pitch angle is given with:

$$G_{\theta,\theta_r}(s) = \frac{\theta(s)}{\theta_r(s)} = \frac{C_1(G_1 - C_2G_2)}{1 + C_1(G_1 - C_2G_2)}. \tag{3}$$

First, we compute the static gain of (3) to show that the MMC-VPC controller ensures zero static error given a reference:

$$\lim_{s->0} G_{\theta,\theta_r}(s) = \lim_{s->0} \frac{C_1}{\frac{1}{(G_1 - C_2G_2)} + C_1} = 1, \tag{4}$$

where we used $\lim_{s->0}(G_1 - C_2G_2) = \infty$, as the transfer functions G_1 and G_2 have infinite gain and C_2 is chosen as a negative I controller. As both G_1 and G_2 have positive gains, the gain of C_2 is chosen negative to ensure that the moments produced by CoG variations and rotors' variations have the same direction. Next, we compute closed loop transfer function of $x_{ref}(s)$ given an output

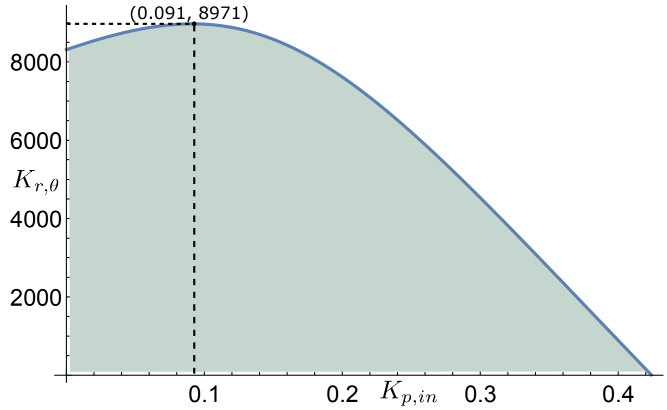

Fig. 3: Stability region (green color) of the MMC-VPC structure, as a function of the controllers' gains Kp_{in} (proportional gain of the main controller) and $K_{r,\theta}$ (integral gain of the auxiliary controller). The curve determining the region has been determined analytically through the Routh-Hourwitz analysis.

reference $\theta_r(s)$ and its static gain:

$$\begin{aligned} G_{x_c,\theta_r}(s) = \frac{x_{ref}(s)}{\theta_r(s)} &= \frac{C_1}{1 + C_1(G_1 - C_2G_2)} \\ &= C_1(1 - G_{\theta,\theta_r}(s)), \end{aligned} \tag{5}$$

$$\lim_{s->0} G_{x_c,\theta_r}(s) = 0. \tag{6}$$

Finally, we compute the transfer functions and static gains of the output value θ and CoG position reference x_{ref} given an output disturbance d:

$$\begin{aligned} G_{\theta,d}(s) = \frac{\theta(s)}{d(s)} &= \frac{1}{1 + C_1(G_1 - C_2G_2)} \\ &= (1 - G_{\theta,\theta_r}(s)), \end{aligned} \tag{7}$$

$$\lim_{s->0} G_{\theta,d}(s) = 0, \tag{8}$$

$$\begin{aligned} G_{x_{ref},d}(s) = \frac{x_{ref}(s)}{d(s)} &= \frac{C_1}{1 + C_1(G_1 - C_2G_2)} \\ &= C_1(1 - G_{\theta,\theta_r}(s)), \end{aligned} \tag{9}$$

$$\lim_{s->0} G_{x_c,\theta_r}(s) = 0. \tag{10}$$

The computed steady state gains prove that the proposed MMC-VPC structure ensures reference tracking and output disturbance rejection with zero steady CoG position, which allows the moving mass mechanism to work around the center point of this operating range.

B. Stability and gain design

The final required property of the MMC-VPC structure is system stability. Alongside the stability, we also consider the controller parameters' design in continuous time domain. To that end, we analyze the stability of the angular rate control loop, which is the inner loop of the cascade P-P structure. In this section, we give the analysis for pitch control, and the same procedure is repeated for roll control. We obtain the characteristic polynomial as the nominator of $1 + C_1(G_1 - C_2G_2)$.

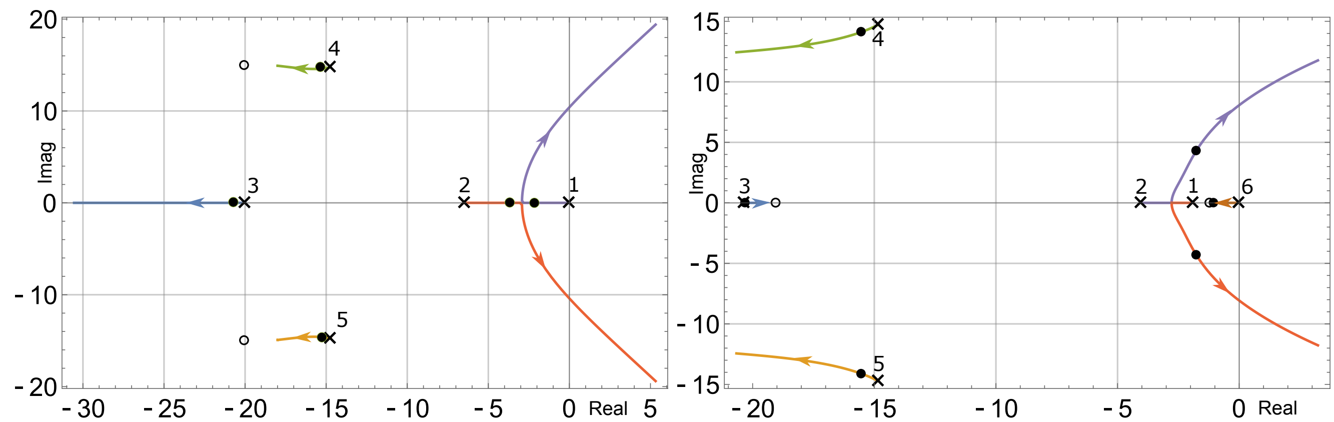

(a) Inner control loop.

(b) Outer control loop.

Fig. 4: Root locus curves used to determine the controller's gains. In the left figure we show the curve of the inner control loop (angular rate) as a function of the $K_{r,\theta}$. Proportional gain is chosen as the value for which the stability curve attains its maximum ($K_{p,in} = 0.091$, see Fig 3). On the right figure, the root-locus curve for the outer control loop (angle) is shown, which is a function of the proportional gain Kp_{out}. Black dots represent the chosen poles.

If we use PT_2S model for the moving mass dynamics [7], we obtain a fifth order polynomial. Using a Routh-Hourwitz criterion we obtain constraints for controllers' gains in the form $K_{r,\theta} < f(Kp_{in})$, $Kp_{in} > 0$ & $Kp_{in} < 0.424$, $K_{r,\theta} > 0$, where $f(Kp_{in})$ is given as a real root of a polynomial function. Since it is not convenient to explicitly express function $f(Kp_{in})$, we give its graphical representation in Fig. 3. For the chosen proportional gain of the main controller, from the figure we obtain the limit on the integral gain of the auxiliary controller. It can be noticed that the function $f(Kp_{in})$ has a local extremum $(Kp_{in,e}, K_{r,\theta,e}) = (0.091, 8971)$, which means that for $0 < Kp_{in} < Kp_{in,e}$, the integral gain limit increases as the proportional gain increases, while increasing Kp_{in} above $Kp_{in,e}$ decreases the integral gain limit. For the proposed structure, it is beneficial to use higher integral gain value as it leads to faster dynamics of the moving masses reaching a desired steady state. Results obtained from Routh-Hurwitz analysis suggest that, if we increase integral gain value of the auxiliary controller, we should also increase proportional gain of the main controller, but only up to $Kp_{in,e}$, for which we get the biggest stability margin. Therefore, we propose to choose $Kp_{in} = Kp_{in,e}$ as the proportional gain for the inner cascade loop, and to determine $K_{r,\theta}$, we use root-locus curve to place the poles of the angular rate control loop. The curve is given in Fig. 4a, and we choose $K_{r,\theta} = 500$ which gives a pair of real poles that dominate system dynamics. Finally, we design the proportional gain Kp_{out} of the outer loop of the main controller. The corresponding root locus curve is given in Fig. 4b, from which we choose $Kp_{out} = 2.0$ (the closed loop poles are marked with black dots).

IV. Simulation

To validate the MMC-VPC concept, we created a realistic simulation environment in Gazebo simulator within Robot Operating System (ROS). We model the UAV as a single rigid body with rotating joints attached to each of four motor arms. Furthermore, each rotating joint has a propeller attached. In order to simulate rotor dynamics we use a plugin from open source *rotors_simulator* [14] package. We also equip the UAV with realistic sensors from *hector_gazebo* [15] to measure vehicle's attitude and pose.

We test pitch reference tracking and stabilization of a basic MMC controller (P-P cascade) and a MMC-VPC controller under disturbances. The controllers' parameters are designed in the previous section. Note that we only show results for the pitch degree of freedom, but similar results are obtained for the roll axis as well. The simulation responses are given in Fig. 5a and Fig. 5b.

We include disturbances in the form of unmodelled dynamics and external moments applied to the vehicle body. The first disturbance is produced by a rotor flapping force acting on some radius from CoG. The flapping force is proportional to rotor speed and vehicle's linear velocity. As the vehicle tilts and starts translating, the moment produced by the rotor flapping force opposes the moments that produced the tilting of the vehicle, thus acting as a drag moment. Since this moment is proportional to the vehicle's linear velocity, the moment varies as the vehicle accelerates/decelerates [1],[16]. Therefore, if we only use a cascade P-P controller for roll/pitch control (basic MMC control), we obtain a steady state angle error (first part of the Fig. 5a), and a non-zero steady state moving mass position (Fig. 5b). While a steady state error could be diminished by adding an integral component in the cascade controller, a non-steady state moving mass position can not be avoided. Next, we simulate a disturbance acting on the vehicle for several seconds as a constant external moment (0.1 Nm). This disturbance presents a model of wind gusts that can be expected during outdoor flights. The response of the vehicle's pitch angle and moving mass position are shown in the second part of the Fig. 5a and Fig. 5b, respectively. While the disturbance is active (period 40-47 sec), there is a constant pitch error in the attitude response, and the moving masses are displaced away from their initial position.

We repeat the same experiments with the vehicle controlled by the proposed MMC-VPC structure. The responses of the pitch angle and the moving mass position are presented in the third and fourth part of the Fig. 5a and Fig. 5b, respectively. In Fig. 5b we also show rotors' variations commanded by the VPC part of the algorithm. It can be noticed that the MMC-VPC controller results in the zero steady state angle error and zero steady state moving mass position under both disturbances produced. This is achieved by commanding rotors' variations that diminish the influence of disturbances, which eventually leads the moving masses to the center position, and ensures zero steady state angle error. The presented results confirm the findings obtained in the previous section from the transfer functions analysis, and also suggest increased robustness of the MMC-VPC structure over basic MMC controller.

V. Experiments

To demonstrate the proposed MMC-VPC control algorithm in action, we present the experimental results conducted on a real physical platform μMORUS, shown in Fig. 1. Our aerial robot is an ArduCopter quadrotor equipped with two moving masses (NEMA 14 stepper motors) with a rack and pinion mechanism that transform rotational motion into linear motion. Masses are placed only on the x-axis, which allows to control the pitch angle through MMC and MMC-VPC concepts. At the same time, the rotors are symmetrically placed around the central body in a pattern known as plus (+) configuration. We use a custom designed printed circuit board to command stepper motors and Pixhawk PX4 as the flight controller. MMC-VPC control algorithm is implemented on off-board computer within ROS. The same off-board computer is used for data logging. For testing purposes μMORUS is powered over electric cables and connected to the off-board computer through a USB cable.

In this paper we present the experiments of the μMORUS vehicle mounted on a 2DOF gimbal, which allows to control the pitch and yaw angles. We use the gimbal to test and tune control algorithms until satisfactory attitude response is achieved. The sequence of commanded references and the response of vehicle's pitch angle are presented in Fig. 6a. The MMC-VPC algorithm output is given in Figure. 6b. Measured attitude data shows satisfying command tracking performance with RMS error of 0.038 rad, average overshoot of 27.5% and average rise time $t_r = 0.32$ s. The measured overshoot is partially caused by system zeros (see Egu. 1), and thus can be reduced by including a low-pass filter on the angle reference. The noise in moving masses motion is caused by rotor vibrations and unmodelled dynamics. Since we have shown that the moving masses are operating in higher bandwidth, they are responsible for initial, transient response, which one can observe in Fig. 6b. After certain amount of time, the MMC-VPC controller adjusts rotors' speed and the masses return to the center point of their operating range. This is identical to the results shown and discussed in Section IV, and derived in Section III. In [17] we show a video footage of the experiments, where one can also see a successful flight of the μMORUS vehicle. The analysis of the flight results goes beyond the scope of this paper.

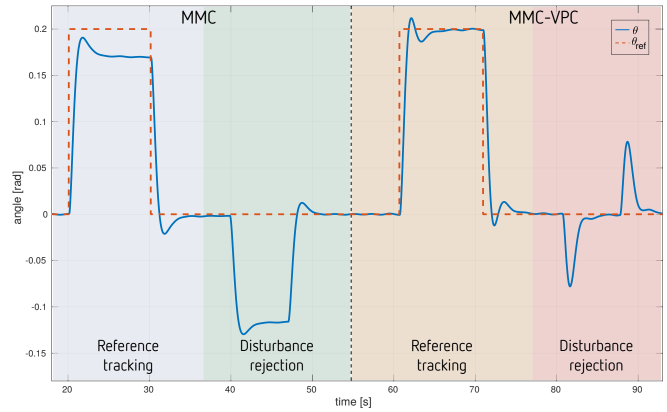

(a) Pitch angle response.

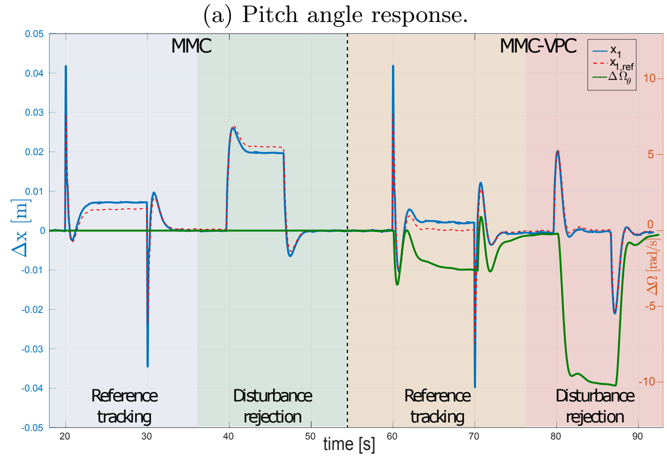

(b) Moving mass and rotors response.

Fig. 5: Simulation results of the UAV equipped with four moving masses. We test vehicle performance under MMC control (first and second part of the response), and MMC-VPC control (third and fourth part). In (a) we show the response of the desired and measured pitch angle, and in (b), the response of the moving mass reference and measured position is shown. In (b) we also show the output of the VPC part of the controller, which is the command for rotors 1 and 3 speed variations.

VI. Conclusion

In this paper we propose MMC-VPC attitude control for UAVs. The approach utilizes both shifting of the vehicle's CoG and variations of rotors' angular velocity.

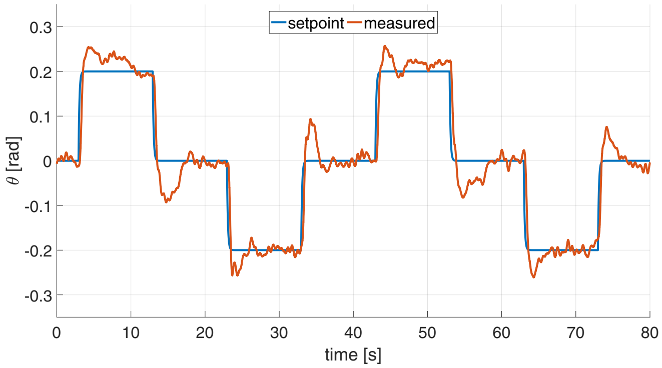

(a)

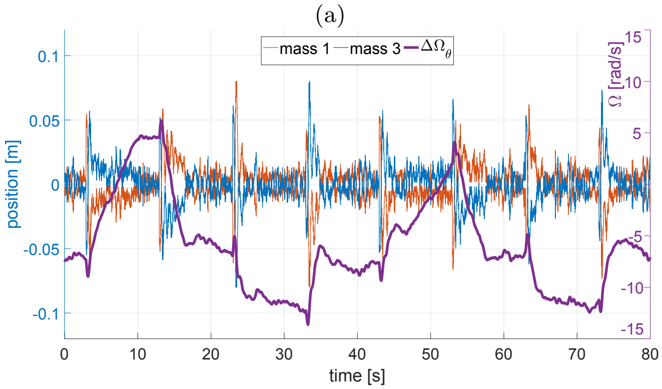

(b)

Fig. 6: Experimental results of μMORUS UAV on gimbal. a) shows a sequence of pitch references and the corresponding responses. b) shows a position setpoint of the moving masses and MMC-VPC control algorithm output for rotors.

Through the transfer function analysis, we have shown that the concept ensures vehicle stability, reference tracking and disturbance rejection. Furthermore, we have shown through the Routh-Hurwitz criterion and root-locus analysis how to properly choose the controller's gains in order to increase the stability margin. In simulation environment, we have successfully tested the proposed control strategy for quadcopter equipped with four moving masses. We have shown that the moving masses operate on higher bandwidth, changing the vehicle's CoG, thus enabling fast change of attitude. At the same time rotors operate on lower bandwidth, making sure the moving masses avoid saturation limits, which is the key benefit of this control strategy. In experimental setup, we tested the control approach on μMORUS UAV mounted on a 2DOF gimbal, and obtained the results that comply with the presented mathematical analysis and simulation results. In our future work we plan to utilize the same concept for attitude control on the heavy-lift MORUS UAV that we are currently building.

ACKNOWLEDGMENT

This research was supported in part by NATO's Emerging Security Challenges Division in the framework of the Science for Peace and Security Programme as Multi Year Project under G. A. number 984807, named Unmanned system for maritime security and environmental monitoring - MORUS.

References

[1] R. E. Mahony, V. Kumar, and P. Corke, "Multirotor aerial vehicles: Modeling, estimation, and control of quadrotor," *IEEE Robot. Automat. Mag.*, pp. 20–32, 2012.

[2] T. Hamel, R. Mahony, R. Lozano, and J. Ostrowski, "Dynamic modelling and configuration stabilization for an x4-flyer," *IFAC Proceedings Volumes*, vol. 35, no. 1, pp. 217 – 222, 2002. 15th IFAC World Congress.

[3] D. Mellinger, Q. Lindsey, M. Shomin, and V. Kumar, "Design, modeling, estimation and control for aerial grasping and manipulation," in *Proc. IEEE/RSJ Int Intelligent Robots and Systems (IROS) Conf*, pp. 2668–2673, 2011.

[4] C. Korpela, M. Orsag, and P. Oh, "Towards valve turning using a dual-arm aerial manipulator," in *2014 IEEE/RSJ International Conference on Intelligent Robots and Systems*, pp. 3411–3416, Sept 2014.

[5] M. Fumagalli, R. Naldi, A. Macchelli, R. Carloni, S. Stramigioli, and L. Marconi, "Modeling and control of a flying robot for contact inspection," in *Intelligent Robots and Systems (IROS), 2012 IEEE/RSJ International Conference on*, pp. 3532–3537, 2012.

[6] A. Jimenez-Cano, J. Martin, G. Heredia, A. Ollero, and R. Cano, "Control of an aerial robot with multi-link arm for assembly tasks," in *Robotics and Automation (ICRA), 2013 IEEE International Conference on*, pp. 4916–4921, May 2013.

[7] T. Haus, M. Orsag, and S. Bogdan, "Mathematical Modelling and Control of an Unmanned Aerial Vehicle with Moving Mass Control Concept," *Journal of Intelligent and Robotic Systems: Theory and Applications*, 2017.

[8] T. Haus, M. Car, M. Orsag, and S. Bogdan, "Identification results of an internal combustion engine as a quadrotor propulsion system," in *2017 25th Mediterranean Conference on Control and Automation (MED)*, pp. 713–718, July 2017.

[9] B. J. Allison and A. J. Isaksson, "Design and Performance of Mid-Ranging Controllers," *IFAC Proceedings Volumes*, vol. 30, no. 9, pp. 523–528, 1997.

[10] B. J. Allison and S. Ogawa, "Design and tuning of valve position controllers with industrial applications," *Transactions of the Institute of Measurement and Control*, vol. 25, no. 1, pp. 3–16, 2003.

[11] O. Sornmo, B. Olofsson, A. Robertsson, and R. Johansson, "Adaptive internal model control for mid-ranging of closed-loop systems with internal saturation," *IEEE International Conference on Intelligent Robots and Systems*, pp. 4893–4899, 2013.

[12] Z. Ma, G. S. Hong, M. H. Ang, and A. N. Poo, "Mid-ranging control of a macro/mini manipulator," in *2015 IEEE International Conference on Advanced Intelligent Mechatronics (AIM)*, pp. 755–760, July 2015.

[13] T. Haus, M. Orsag, and S. Bogdan, "A concept of a non-tilting multirotor-uav based on moving mass control," in *2017 International Conference on Unmanned Aircraft Systems (ICUAS)*, pp. 1618–1624, June 2017.

[14] F. Furrer, M. Burri, M. Achtelik, and R. Siegwart, *Robot Operating System (ROS): The Complete Reference (Volume 1)*, ch. RotorS—A Modular Gazebo MAV Simulator Framework, pp. 595–625. Cham: Springer International Publishing, 2016.

[15] J. Meyer, A. Sendobry, S. Kohlbrecher, U. Klingauf, and O. von Stryk, "Comprehensive simulation of quadrotor uavs using ros and gazebo," in *3rd Int. Conf. on Simulation, Modeling and Programming for Autonomous Robots (SIMPAR)*, p. to appear, 2012.

[16] R. Leishman, J. Macdonald, R. Beard, and T. McLain, "Quadrotors and accelerometers: State estimation with an improved dynamic model," *Control Systems, IEEE*, vol. 34, pp. 28–41, Feb 2014.

[17] "Laboratory for robotics and intelligent control systems youtube channel." `https://goo.gl/1PWUJ2`. Accessed: 2018-02-23.